PHYSICAL REVIEW B VOLUME 16, NUMBER 12 15 DECEMBER 1977

Anisotropic x-ray absorption in layered compounds*

Steve M. Heald and Edward A. Stern
Department of Physics, University of Washington, Seattle, Washington 98195
(Received 18 July 1977)

A study is presented of anisotropy effects in x-ray absorption in the layered compounds of $2H$-WSe_2 and $1T$-TaS_2. In the measurements it was essential to separate the thickness effect from the true anisotropy effect which is dependent on the angle between the x-ray polarization and the crystal axes. The Se K edge and the W and Ta L edges were measured. Anisotropy in the white line of Se was found but no anisotropy was discerned in the W and Ta white lines. It is pointed out that x-ray absorption in general, and the extended x-ray absorption fine structure (EXAFS) in particular, have the anisotropy dependence of a second-order tensor and the theoretical expression for the EXAFS anisotropy at the $L_{2,3}$ edges is explicitly displayed. The anisotropy of the EXAFS in the Se and W absorption was measured and a good agreement with theory is found. The anisotropy of EXAFS at the $L_{2,3}$ edges has the new feature of a cross term between the final s and d states, which permits a determination from the measurements that the average contributions of the final s state is 0.02 of that of the final d states to the total absorption of the W L_3 edge. Finally, only qualitative agreement is obtained between band calculations and the near edge x-ray absorption structure, as expected theoretically.

I. INTRODUCTION

Recent developments in the analysis of the extended x-ray absorption fine structure (EXAFS) above x-ray absorption edges have shown it to be an exciting new source of information about atomic structure. Also present near the K and L absorption edges of many elements are large peaks or "white lines" in the x-ray absorption coefficients. These white lines are known to be due to transitions of the initial s and p electrons to a high density of final states which is due to band-structure or excitonic effects. Traditionally the study of absorption edges has been used to infer information about the electronic environment of the material.[1] A recent quantitative study of the white line in platinum[2] has shown that much information can be inferred concerning the nature of the electronic band structure near the Fermi level.

For anisotropic materials both the local atomic and electronic structure will be anisotropic, and it might be expected that this anisotropy will be exhibited in both the white line and EXAFS as the direction of the x-ray polarization vector is varied. In this paper, we study this effect for the anisotropic materials $1T$-TaS_2 and $2H$-WSe_2. These materials are members of a class of transition-metal-dichalcogenide compounds which have attracted a great deal of interest recently for their quasi-two-dimensional structure, and the existence of charge-density waves in several of them. They consist of a layer of transition-metal atoms covalently bonded between two layers of chalcogen atoms. The covalently bonded sandwiches are bound into a three-dimensional structure by weak Van der Waals forces. Thus, intralayer interactions are much stronger than interlayer interactions, leading to highly anisotropic properties.

The x-ray absorption edges of several of these layered materials have been measured,[3,4] but only in our previous measurements[5] on $1T$-TaS_2 was an attempt made to study anisotropy. An apparent anisotropy was found in the Ta L_3 edge. In the present work the Ta L_2 and L_3 white lines were again studied in $1T$-TaS_2 as the angle of the x-ray polarization vector with respect to the normal of the planes was varied from 90° to 43°. No dependence of the strength of the white lines on angle was found. This contradicts our previous measurements and it will be shown that the apparent anisotropy was due to inadequate consideration of simple-thickness effects.

In $2H$-WSe_2, extensive measurements were made of the W L_2 and L_3 and Se K edges. Again no anisotropy of the white line was found for the W edges. However, in the Se K edge a true anisotropy was found, with both the strength and position of the wnite line being dependent on the x-ray polarization direction. Possible thickness effects are ruled out experimentally by independently varying the thickness of the samples. For the W L_3 and Se K edges the EXAFS were also measured as a function of polarization direction. In both cases anisotropy was observed which can be related to the known structural anisotropy of this material.

Previous studies of anisotropy in EXAFS have been limited to the K edge.[6,8] In this paper we also measure anisotropy in the L edge and derive, for the first time, explicit expressions for the angular dependence of EXAFS for this edge. In particular, we point out that x-ray absorption has the anisotropy of a second-rank tensor, a fact

that does not seem to be appreciated before, explaining why cubic crystals show no true anisotropy.[6]

The organization of this paper is as follows. Section II reviews the theoretical basis for anisotropy in both white lines and EXAFS. In Sec. III thickness effects and their bearing on these measurements are discussed. The data listed in the preceding paragraph are presented in Sec. IV. The various facets of these data are then individually analyzed in Sec. V, and the results are summarized in the final section.

II. ANISOTROPY

A calculation of the angular dependence of the EXAFS can proceed in two different ways. The first approach is to make use of the well-known symmetry properties of the crystal and x-ray absorption coefficient to determine the allowed angular dependence of the absorption.[7] We will call this approach the macroscopic theory. The second approach, called the microscopic theory, involves using the explicit angular dependence of the initial and final states to calculate the angular dependence of the EXAFS. This has already been done for absorption at the K edge,[9] and we will carry out the same calculation here for the $L_{2,3}$ edge.

The x-ray absorption coefficient μ can be described in terms familiar in the optical range of the electromagnetic spectrum. In the x-ray regime where the real part of the dielectric constant is very close to one, the relation holds that

$$\mu = (\omega/c)\epsilon_2 , \tag{1}$$

where ω is the radial frequency of the x ray, c is the velocity of light, and ϵ_2 is the imaginary part of the dielectric constant. The local or dipole approximation for the dielectric constant holds for the x-ray region. Equation (1) shows that μ has the same transformation properties with respect to the crystal axes as does the dielectric constant, namely, that of a second-rank tensor.

It follows from this that for cubic or higher symmetry μ is independent of orientation of the crystal axes. One requires lower than cubic symmetry for an angular dependence. In the case of the layered compounds with threefold or higher symmetry about the normal to the layers, a straightforward calculation using the macroscopic theory shows that μ will have no dependence with polarization in the layered planes and will vary as

$$\mu(\theta) = \mu_{\parallel} + (\mu_{\perp} - \mu_{\parallel})\cos^2\theta , \tag{2}$$

where θ is the angle between the polarization vector and the normal to the layered planes, and $\mu_{\parallel}$ and $\mu_{\perp}$ are the absorption coefficients with the polarization vector parallel and perpendicular to the layers, respectively.

An isolated atom on the average has no orientation dependence in its absorption. The interactions with the surrounding atoms produces the orientation dependence. Offhand, it is not obvious that the microscopic theory will give the same results as the above macroscopic theory. Absorption at the $L_{2,3}$ edge involves transitions from initial p states to final s and d states. The s states give no orientational dependence, but d states can have a complicated angular dependence.

It follows from the microscopic theory[9] that EXAFS at the $L_{2,16}$ dge has a contribution from the final d states of the form

$$\chi_2'(k) = \sum_{m=0}^{1}\sum_i D_m(R_i, k)\, Y_{2,m}^*(-\hat{r}_i)\, Y_{2,m}(\hat{r}_i) , \tag{3}$$

where $Y_{2,m}(\hat{r}_i)$ is the spherical harmonic for a d state with a component of angular momentum evaluated in the direction $\hat{r}_i$, the direction from the center atom to the ith atom and D_m has no angular dependence. Each one of the terms in (3) has trigonometric functions to the fourth power, instead of to the second power, as required by the macroscopic theory. The paradox is resolved by the sum of the terms reducing to the required second power, even though each term is a higher power. In addition to the diagonal terms there are also cross terms[8] coupling $Y_{2,0}$ and Y_{00} but this product is already second order and poses no difficulty.

Evaluating the terms from the microscopic theory with the z direction along the x-ray polarization, one obtains

$$\begin{aligned}\chi(k) = \Bigg(& \langle 1|2\rangle\langle 0|1\rangle \sum_i \frac{\sin[2kR_i + \delta_{02}'(k)]}{kR_i^2} |f_i(k)| (1 - 3\cos^2\theta_i) \\ & + \frac{|\langle 2|1\rangle|^2}{2} \sum_i \frac{\sin[2kR_i + \delta_2'(k)]}{kR_i^2} |f_i(k)| (1 + 3\cos^2\theta_i) \\ & + \frac{|\langle 0|1\rangle|^2}{2} \sum_i \frac{\sin[2kR_i + \delta_0'(k)]}{kR_i^2} |f_i(k)| \Bigg) (|\langle 2|1\rangle|^2 + \tfrac{1}{2}|\langle 0|1\rangle|^2)^{-1} ,\end{aligned} \tag{4}$$

where $\langle l|1\rangle$ is the matrix element of the radial portions of the wave functions between the excited state of angular momentum l and the initial $2p$ state, $|f_i(k)|$ is the magnitude of the backward-scattering amplitude from the ith atom at $\vec{R}_i$, θ_i is the angle between the polarization direction and the line between the center atom and the ith atom, k is the wave number of the photoelectron and

$$\begin{aligned}\delta_2'(k) &= 2\delta_2 + \delta\,,\\ \delta_0'(k) &= 2\delta_0 + \delta\,,\\ \delta_{02}'(k) &= \delta_2 + \delta_0 + \delta\,.\end{aligned} \tag{5}$$

Here δ_l is the phase shift of the partial wave of angular momentum l introduced by the central potential, and δ is the phase shift associated with $f_i(k)$, i.e.,

$$f_i(k) = |f_i(k)|e^{i\delta(k)}\,. \tag{6}$$

It is clear that the $\chi(k)$ of (4) will have the orientation dependence required by the macroscopic theory. One can utilize the orientation dependence measured from experiment to estimate the ratio $\langle 0|1\rangle/\langle 2|1\rangle$, as we do below.

III. THICKNESS EFFECTS

As mentioned in the introduction, when measuring the strength of white lines one has to be very careful to rule out spurious variations due to changes in the sample thickness. This fact has been known since early studies of white lines[10] and is known as the thickness effect. It has its origin in the fact that even a supposedly monochromatic x-ray source can contain wavelengths well away from the central peak. While these may comprise only a very small percentage of the incoming x-ray beam, after being attenuated by a strong absorption white line the transmitted beam may be dominated by the impurity wavelengths. To illustrate this problem a simple calculation is useful. Suppose one wants to measure a step in the absorption structure which has a total absorption change $\Delta\mu$. Then if I_1 and I_2 are the intensities just before and after the step one can write

$$\Delta\mu x = \ln(I_1/I_2) \tag{7}$$

for a sample of uniform thickness x. We now allow a leakage intensity $I_L = fI_1$, defined as any transmitted radiation which is unaffected by the changes in $\Delta\mu$. It can be due to sources such as the tails of the monochromator transmission function, harmonics from the monochromator or leakage through cracks and pinholes in the sample. The measured absorption step will then be

$$\Delta\mu' x = \ln\frac{I_1 + fI_1}{I_2 + fI_1} = \ln\frac{1+f}{e^{-\Delta\mu x} + f}\,. \tag{8}$$

Clearly the measured absorption step will approximately equal the actual step only if $e^{-\Delta\mu x} \gg f$.

For the present measurements there can be several contributions to f which are difficult to estimate. Therefore, experimentally varying the thickness of the samples is the only reliable method for determining the thickness effects. This is especially necessary for anisotropy measurements since the samples must be rotated in order to change the direction of the x-ray polarization with respect to the crystal layers. Such a rotation changes the thickness of the sample presented to the x-ray beam and can cause corresponding changes in the strength of the white line. An example of the dependence of a white line on sample thickness is shown in Fig. 1 for tantalum metal 5, 10, and 15 μm thick. These results were obtained on the same experimental setup at the Stanford Synchrotron Radiation Project (SSRP) as the measurements on the layered compounds to be described, and thus represent a good estimate of the magnitude of the thickness effect for the present experimental conditions.

The geometry used for measuring the absorption of the layered compounds is shown in the inset to Fig. 4. The samples are cleaved to a thickness of a few microns and then carefully masked with lead to prevent any leakage of radiation around the sample. The c axis (perpendicular to the layers) is along the thin direction. The x rays at SSRP are almost completely polarized in the horizontal plane. Therefore, rotation about the vertical axis (θ) changes the direction of the polarization vector with respect to the crystal layers. Rotation about that horizontal axis parallel to the polarization (ϕ) causes the thickness of the sample to change but

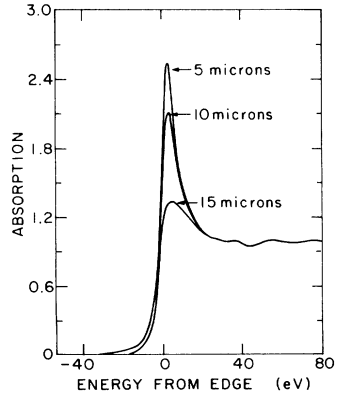

FIG. 1. Dependence of the white line on sample thickness for pure tantalum. The different thickness have all been normalized to an absorption step of 1. A thickness of 4 μm has an absorption step of 1.

TABLE I. Data from $1T$-TaS_2 for the tantalum L_2 and L_3 edges. R is the ratio of the absorption at the white line maximum to the absorption step at the edge.

Rotation angles		Step $\Delta\mu x$	R
		L_3 edge	
$\theta=0$	$\phi=0$	0.938 ± 0.005	2.94 ± 0.025
$\theta=0$	$\phi=45$	1.416 ± 0.005	2.80 ± 0.025
$\theta=45$	$\phi=0$	1.306 ± 0.005	2.90 ± 0.025
		L_2 edge	
$\theta=0$	$\phi=45$	$0.67\ \pm0.01$	2.99 ± 0.06
$\theta=45$	$\phi=0$	$0.59\ \pm0.01$	3.11 ± 0.06

leaves the angle of the polarization vector unchanged with respect to the crystal layers. A true anisotropy is a change which shows up in a θ rotation and does not show up in a corresponding ϕ rotation.

IV. EXPERIMENTAL RESULTS

The measurements were performed on SSRP EXAFS line No. 2 in the manner described in the previous section. The energy resolution was about 2 eV. The Ta L_2 and L_3 edges were studied in $1T$-TaS_2 as a function of angle, and in Ta metal as a function of thickness as just described. The W L_2 and L_3 and Se K edges were studied in $2H$-WSe_2 as a function of polarization angle. In addition, EXAFS for both the W L_3 and Se K edges was measured. The results for the layered compounds are presented below.

$1T$-TaS_2

Table I lists the results obtained on the L_2 and L_3 white lines. Listed in this table are the jump at the step, which indicates the effective thickness of the sample, and the ratio R, which is the ratio of the white line peak to the step. These results were obtained after subtracting off the slowly varying background absorption before the step. The errors were estimated by adding the estimated contributions from three sources: the error due to the background subtraction, the error in locating the peak maximum, and the error in finding the step height. The data for the L_2 edge is less accurate because the background absorption before the edge was not well determined. The fact that $\Delta\mu x$ at the step for both of the 45° rotations is approximately $\sqrt{2}$ times $\Delta\mu x$ for the step at normal ($\theta=0$, $\phi=0$) incidence indicates that the sample is reasonably uniform in thickness.

To determine the important of thickness effects the ratio R versus $\Delta\mu x$ at the step is plotted in Fig. 2 for both $1T$-TaS_2 and Ta metal. In this plot we see that below $\Delta\mu x \sim 1.5$ the variation of R with sample thickness is small. Also the thickness variation of the $1T$-TaS_2 points is in good agreement with that of Ta metal in spite of the fact that they were taken at varying polarization angles. Thus, we can conclude that, within the experimental accuracy, there is no dependence of the white line strength on the direction of the x-ray polarization direction for both the L_2 and L_3 edges.

It is also interesting to compare the shape of the white line in $1T$-TaS_2 with that of Ta metal. These are shown in Fig. 3 along with the platinum L_2 edge which is an example of a similar edge without a white line. The Ta metal edge is basically a single, somewhat asymmetric peak. For the Ta L_3 white line in $1T$-TaS_2 the leading edge is similar, but the high-energy side of the peak has a shoulder. This feature is independent of

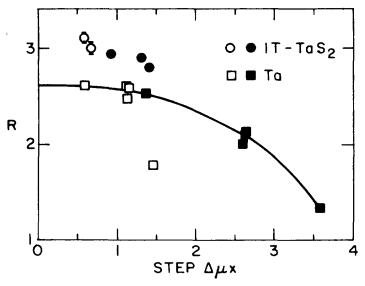

FIG. 2. Variation of the white-line-height ratio R with sample thickness for both Ta and $1T$-TaS_2. Solid symbols refer to the L_3 edge and open symbols to the L_2 edge. The smooth curve for the Ta results is drawn only as a guide to the eye. The reason for the anomalous Ta L_2-edge point is not known.

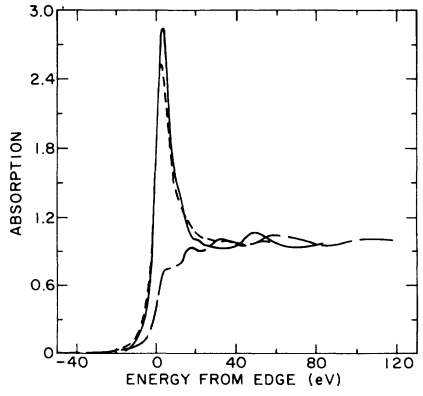

FIG. 3. Comparison of the L_3-edge white lines for pure tantalum (short dashed line) and tantalum in $1T$-TaS_2 (solid line). The platinum L_2 edge (long dashed line) is used as an example of a similar edge with no white line. In all three cases the data have been normalized to an absorption step of 1.

TABLE II. Data from $2H$-WSe_2 for the tungsten L_2 and L_3 edges.

Angle θ	Step $\Delta\mu x$	R
	L_3 edge	
0	0.196 ± 0.002	3.02 ± 0.06
0	0.175	3.18
20	0.208	2.99
20	0.208	3.01
47	0.243	3.08
47	0.251	3.01
	L_2 edge	
0	0.078 ± 0.002	3.32 ± 0.09
47	0.113	3.09

TABLE III. Data from $2H$-WSe_2 for the selenium K edge.

Rotation angles θ	ϕ	Step $\Delta\mu x$	R
0	0	0.209 ± 0.004	1.33 ± 0.03
0	0	0.193	1.36
0	38	0.243	1.36
0	45	0.239	1.41
20	0	0.217	1.28
30	0	0.223	1.29
40	0	0.246	1.23
47	0	0.259	1.22
47	0	0.264	1.20
47	0	0.250	1.19

polarization direction, and will be discussed further in the next section along with the fact that the magnitude of the white line for $1T$-TaS_2 is larger than in the metal.

$2H$-WSe_2

Extensive data were taken for both the W and Se edges in $2H$-WSe_2. The results for the W L_2 and L_3 edges are shown in Table II. Since $\Delta\mu x \sim 0.2$, any thickness effects are negligible, and no rotations about the horizontal axis (ϕ) were taken. For the L_3 edge, two measurements were taken for each of the angles $\theta = 0°$, 20°, 47°. Within the scatter of the points no anisotropy is indicated. Similar results are shown for the L_2 edge at 0° and 47°, although again these measurements are less accurate, this time because of instrumental noise in the vicinity of the edge.

The first true anisotropy of a white line was found in the Se K edge. Figure 4 compares the results obtained for three cases: (a) x-ray polarization vector along the direction of the crystal layers, (b) x-ray polarization vector along the layers, but the thickness has been increased by rotation about the horizontal axis ($\phi = 45°$), and (c) x-ray polarization vector rotated out of the plane of the crystal layers by $\theta = 47°$. All of the results have been normalized to a unit step height for comparison. Actually the unnormalized steps in (b) and (c) are roughly $\sqrt{2}$ times that of (a). It is obvious that in (c) there is a reduction of the intensity of the white line which is related to the direction of the polarization vector and not to the sample thickness. Not as obvious in these plots is the fact that in (c) the first absorption peak has shifted slightly towards higher energies relative to the second peak.

Table III summarizes all the results obtained on the Se edge. It shows a fairly smooth variation of R with the angle θ. For the repeated measure-

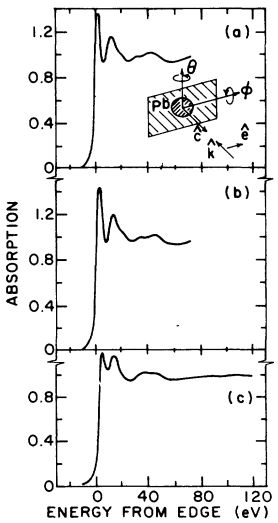

FIG. 4. Anisotropy of the selenium K edge in $2H$-WSe_2. Notice the similarity of (a) and (b) as compared to (c). The inset in (a) shows the geometry of the experiment. $\theta = 0°$ corresponds to the x-ray polarization vector $\hat{e}$ laying in the plane of the crystal layers. $\phi = 0°$ corresponds to the crystal $\hat{c}$ axis laying parallel to the x-ray $\hat{k}$ vector. (a) is for $\theta = \phi = 0°$; (b) is for $\theta = 0°$, $\phi = 45°$; and (c) is for $\theta = 47°$, $\phi = 0°$.

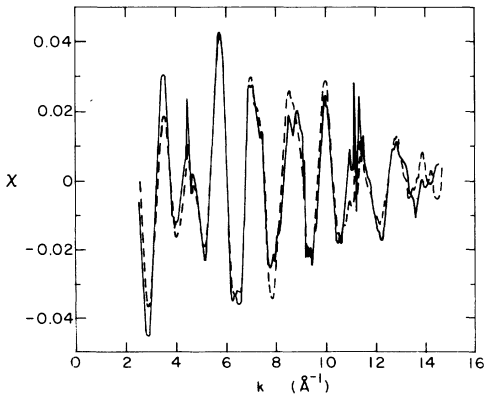

FIG. 5. EXAFS for the tungsten L_3 edge in $2H$-WSe_2. The solid curve is for $\theta = 0°$ and the dashed curve is for $\theta = 47°$.

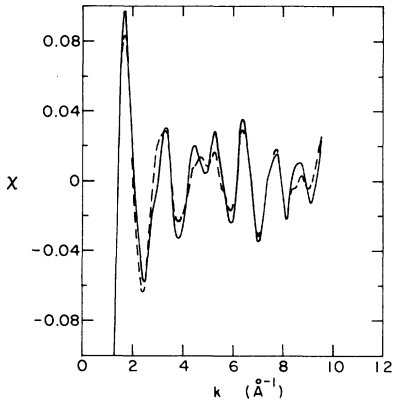

FIG. 6. EXAFS for the selenium K edge in $2H$-WSe_2. The solid curve is for $\theta = 0°$ and the dashed curve is for $\theta = 47°$.

ments at $\theta = 0°$ and $\theta = 47°$ the sample was moved between each to check for the effects of sample inhomogeneity. Although some inhomogeneity is indicated by the varying $\Delta\mu x$, R is nearly constant showing that the effect of inhomogeneity can be neglected. The anisotropy is significantly larger and thus these results represent the first observation of a true anisotropy in a white line, since our new measurements on $1T$-TaS_2 show that the previously reported anisotropy was due to a thickness effect.

The EXAFS was also measured for both the W L_3 and Se K edges as a function of angle, and are shown in Figs. 5 and 6, respectively. In both cases anisotropy is seen as would be expected from the highly anisotropic structure of this material.

V. DISCUSSION

A. Ta and W white lines

Many materials have very strong white lines at the onset of their L absorption edges. As we have seen, tantalum is a good example. These L-edge lines are due to a high density of states with d symmetry just above the Fermi level. Thus, in principle, information about the electronic density of states can be obtained from the white line. This line of research has been pursued for a great many materials and has yielded useful results in some cases. However, there are several complications in these measurements which can make them difficult to interpret and obtain directly the electronic density of states. The most obvious is the fact that the white line is due to partial portions of the density of states, e.g., the s and d part when L_{23} edges are studied. This fact can be used to advantage in isolating the various contributions to the density of states, but must be borne in mind when interpreting the data.

Several other complications are more serious. Lifetime broadening of the short-lived excited state and multielectron effects[11] can smear out its energy by several eV up to tens of eV, with a corresponding loss of resolution of the density of states. In order to obtain the true density of states this broadening must be known in order to deconvolute it from the measured white line. Another serious problem is the fact that the matrix elements governing the white line absorption can be energy dependent. Usually this has the effect of weighting more heavily the lower-energy portion of the band.

A most serious complication, usually ignored, is that when the absorption process occurs a core state is left empty. To the photoelectron the existence of this core hole is much the same as if the Z of the nucleus was raised by 1. The absorbing atom is therefore an impurity imbedded in the solid, and this has to be taken into account when determining what density of states the absorption process is measuring. Current theories assume that the appropriate final state for the system after the x ray is absorbed is one where the electronic wave functions can relax to their configurations in equilibrium with the increased core charge. For such an assumption, the density of states being measured by x-ray absorption is the local density of states at the core hole of the impurity excited atom. Such a local density of states should *not* necessarily have a simple relationship to the density of states of the unperturbed material, even though most investigators assume otherwise. The local density of states is the ordinary density of states weighted by the density of the electronic wave functions of that energy at the point of interest. The density of the wave functions at an excited atom site is expected to be increased over the value of the unperturbed atom at energies just above the Fermi level by the increased positive charge.

With these facts in mind we now turn to the L-edge white lines measured in the present experiment for Ta. From Fig. 3 there is a qualitative difference between the Ta L_3 edge in tantalum metal and $1T$-TaS_2. For tantalum metal the d-symmetric part of the density of states has been determined from band structure calculations.[12] Above the Fermi level it peaks with a width of about 0.5 Ry. In this general peak there are two sharp structures separated by about 0.1 Ry. The measured white line shows only a single somewhat skewed peak with the half width of ~0.7 Ry. There is no quantitative agreement between the density of states of the unperturbed metal and the shape of the white line indicating that the above complica-

tions are significant.

The data for $1T$-TaS_2 do show slight structure in the white line. This can be understood from the band-structure calculations of Mattheis.[13] He finds that the Ta d band is split into two subbands with the Fermi level near the bottom of the lowest-energy subband. The centers of these subbands are about 0.25 Ry apart. The larger separation of these bands and the greater weight in each compared to the sharp structure in Ta metal explains why they are just beginning to be resolved in the white lines, and the data thus lend qualitative support to the band-structure calculations. However, there are still severe quantitative discrepancies.

The weight in the upper band according to band-structure calculations is $\frac{2}{3}$ that of the lower band. Since the Fermi level is in the lower band, the unfilled portions of the bands have equal weights, while in the white line the lower band predominates. This enhancement of the lower band is qualitatively consistent with that expected from a local density of states of the impurity excited atom.

The areas of the white lines were determined using the platinum L_2 edge shown in Fig. 3 as a reference. The white line in $1T$-TaS_2 has approximately 10% more area than the corresponding line in the metal. This means that d states in the vicinity of tantalum are emptied as the compound is formed. Such a result is reasonable since on chemical grounds one would expect some charge transfer from tantalum to sulfur in the formation of the compound.

The white lines at the tungsten L_3 and L_2 edges in $2H$-WSe_2 were also measured. As for tantalum, no dependence on the polarization is found. This might be expected since the local environments of Ta in $1T$-TaS_2 and W in $2H$-WSe_2 are similar. The shape of the white lines is similar to that in tantalum metal with no obvious structure present. Again this result is in qualitative agreement with calculated band structures. In this case we compare to the calculations[13] for $2H$-MoS_2. The band structure for $2H$-WSe_2 should be very similar.[14] For $2H$-MoS_2 the d bands are also split into two subbands, with the lower band containing two d states and the upper the remaining eight d states. However, since $2H$-WSe_2 is a semiconductor the Fermi level falls between these two subbands, and only the upper band would be expected to contribute to the white line.

B. $2H$-WSe_2 Se K edge

To better understand the anisotropy in the Se K-edge white line, a more quantitative measure is helpful. Again we have attempted to determine the area under the white line. In this case, however, the area determination is complicated by the smaller size of the white line and the lack of a good reference edge for the background subtraction. Thus two different backgrounds were used. The first is a straight line connecting the leading edge of the second peak with the onset of the white line. This background is consistent with the assumption that the onset of the edge would be at the same position even if the white line were absent. As such the areas obtained roughly represent lower limits. The true background is likely to rise more steeply which would result in larger areas. To account for this, the second procedure assumes that the leading edge of the white line represents the shape of the background. This would be true if the shapes of both the white line and the hypothetical white line free edge were dominated by instrumental resolution. Such seems to be nearly true for the white line edge. The second choice of a background should give areas which are roughly upper bounds on the true areas.

The results of these two procedures are shown in Fig. 7 for the various measured angles plotted versus $\cos^2\theta$. Two features are worthy of note. As shown in Sec. II the most general angular dependence for absorption is $A + B\cos^2\theta$, and we see that the data are consistent with a linear dependence in $\cos^2\theta$. The peak area at $\theta = 90°$ (intercept A) is seen to be (52–62)% of its value at $\theta = 0$ depending on the assumption used for subtracting off the background. Second, the scatter in the areas as indicated by multiple measurements at $\theta = 47°$ is well inside the angular variation of the area.

Also plotted in Fig. 7 is the position of the peak of the white line relative to the second peak. Again there is consistency with a $\cos^2\theta$ angular dependence, with the white line moving to higher energy as the angle is decreased. The second peak is used as a reference since slippage in the spectro-

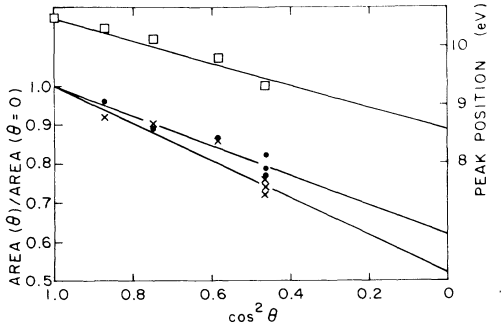

FIG. 7. Angular dependence of the selenium K-edge white line in $2H$-WSe_2. (×): the areas found using the first background subtraction procedure described in the text; (●): the areas found using the second background subtraction procedure; (□): the peak position relative to the second absorption peak.

meter drive rendered absolute energy measurements unreliable. The magnitude and shape of the second peak is independent of angle, and it thus seems likely that its position is also independent of angle. Assuming this to be the case then all of the shifts shown in Fig. 7 are due to movement of the white line, and the peak position shifts about 2 eV to higher energy at $\theta = 90°$.

It is possible to calculate the angular dependence of the strength and position of the white line using the formalism of band-structure calculations. However, such a calculation would not be quantitative since it does not take into account the perturbation introduced by the core hole of the excited atom. In spite of the problems, some qualitative statements can be made using published band structures. Using the usual convention of taking the z axis normal to the planes, when the polarization vector is in the planes, the absorption of the x-ray photon causes the excitation of the electron to a state of p_x or p_y character. Likewise, when the polarization vector is along the z axis p_z states are excited. These facts can be related to the band-structure calculation[13] for $2H$-MoS_2.

From Mattheis' calculation[13] we can compare the relative energy of the bands with p_x, p_y, p_z character just above the Fermi level. This comparison can be done for six symmetry points in the Brillouin zone. For four of the symmetry points there is little separation between bands with p_x, p_y character, and those with p_z character. But for the Γ and A symmetry points the bands with p_z character are substantially higher in energy (~0.3 Ry) than the others. Therefore as the polarization angle θ is increased and the electron is more likely to be excited to states with p_z character, the energy of the white line, which represents an average over all of the Brillouin zone, can be expected to increase, in agreement with our observations.

The fact that both the present experiment and theory indicate that the average energy of the p_z-like states is higher than the p_x and p_y states qualitatively explains the amplitude dependence of the Se white line. As discussed in the previous section on the Ta white line, electronic states can be expected to contribute less to the white line as their energy above the Fermi level increases. The observation of the Se white line amplitude decreasing as its energy increases is consistent with this expectation.

C. $2H$-WSe_2 EXAFS

Since the structure of $2H$-WSe_2 is already well known, the present EXAFS measurements provide no new structural information. However, they can be used to check the expected polarization dependence discussed in Sec. II.

For the Se K edge EXAFS, only p-type states are involved and the expected angular dependence[9] is $\sum_j \cos^2\theta_j$ where θ_j is the angle between the x-

TABLE IV. Anisotropy of the EXAFS for $2H$-WSe_2. For the Se K edge the total angular dependence is calculated. For the tungsten L_3 edge only the second term in Eq. (4) was used in the calculation. The difference of the measured ratio from the calculated ratio is used to calculate the matrix element ratio $\langle 0|1\rangle/\langle 2|1\rangle$.

Neighbor	Distance	Amplitude ($\theta = 0°$)	Amplitude ($\theta = 47°$)	Predicted ratio $\left(\frac{\theta=47°}{\theta=0°}\right)$	Measured ratio $\left(\frac{\theta=47°}{\theta=0°}\right)$
			Se K edge		
W	2.53	0.132	0.169	1.280	1.2 ± 0.2
Se	3.29	0.277	0.135		
Se	3.35	0	0.046		
Se	3.67	0.030	0.098		
W	4.15	0.073	0.050		
Se	4.69	0.067	0.104		

Neighbor	Distance	$\lvert\langle 1\rvert 2\rangle\rvert^2$ term $\left(\frac{\theta=47°}{\theta=0°}\right)$	Measured ratio $\left(\frac{\theta=47°}{\theta=0°}\right)$	$\frac{\langle 0\rvert 1\rangle}{\langle 2\rvert 1\rangle}$
		W L_3 edge		
Se	2.53	1.137	1.08 ± 0.02	0.20 ± 0.06
W	3.29	0.671	0.67 ± 0.15	0 ± 0.5
Se	4.15	0.813		
Se	4.81	2.62		

ray polarization vector and the vector to the jth neighbor. There is also the possibility of an anisotropic Debye-Waller factor, but in general the anisotropy should be dominated by the $\cos^2\theta_j$ factor. This angular dependence is tabulated in Table IV. For the W L_3-edge EXAFS the situation is more complicated since both s- and d-type final states are involved and the dependence is given in Eq. (4). It has been shown for gold[15] that the dominant contribution to the EXAFS comes from the d final states. It is likely that the same is true for tungsten. Assuming that $\langle 0|1\rangle$ in Eq. (4) is small, the $|\langle 2|1\rangle|^2$ term will dominate the angular dependence. The expected ratio of EXAFS at $\theta = 0$ to that at $\theta = 47°$ contributed by this term is tabulated for various shells in Table IV.

We will first consider the Se K-edge EXAFS given in Fig. 6. The Fourier transforms of $k\chi(k)$ are shown in Fig. 8. The peaks in these transforms correspond to the distances given in Table IV shifted by the appropriate phase shifts. The phase shifts are 0.62 ± 0.03 Å for Se-W distances and 0.35 Å ± 0.02 for Se-Se distances. The Se-W phase shift is obtained from the location of the first shell in the present transforms, and the Se-Se phase shift is from pure Se data. The Se-Se phase shift is less accurately obtained directly from the present data because of interference between shells at similar distances. However, the phase shift obtained from pure selenium agrees well with the WSe_2 data.

Comparing the transforms in Fig. 8 it is obvious

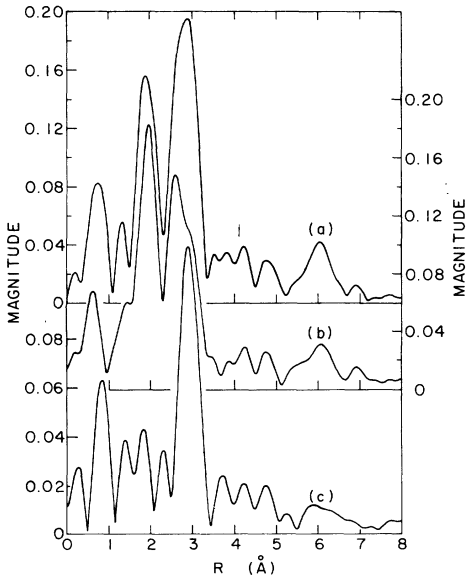

FIG. 8. Magnitude of the Fourier transform of k times the data shown in Fig. 6: (a) $\theta = 0°$, (b) $\theta = 47°$, (c) transform of $\theta = 47°$ data minus 1.2 times the $\theta = 0°$ data. Note the change in scale.

a definite anisotropy exists, which is particularly evident in the second large peak. From Table IV, this second peak is a mixture of unresolved contributions from three separate shells. For $\theta = 0°$ the shell at 3.29 Å provides the dominant contribution and the corresponding peak in the transform shows little sign of the other shells. However, for $\theta = 47°$ all three shells contribute substantially and the transform peak shows obvious signs of interference. Additional differences in the transforms are seen at larger R, but it is difficult to separate real effects from noise in this region.

Because of the interference between closely spaced shells it is difficult to obtain relative amplitudes directly from these transforms. One useful technique is to combine the data taken at $\theta = 0°$ and $\theta = 47°$ before making the transform. For example, if the $\theta = 0°$ data is multiplied by the appropriate factor and subtracted from the $\theta = 47°$ data the contribution from the Se-W shell at 2.53 Å can be cancelled out. The resulting transform will then show no peak due to this shell. This is shown in Fig. 8(c). The factor multiplying the $\theta = 0°$ data which gives the best cancellation of the first shell contribution is 1.2 ± 0.2. This is in good agreement with the predicted ratio 1.28 listed in Table

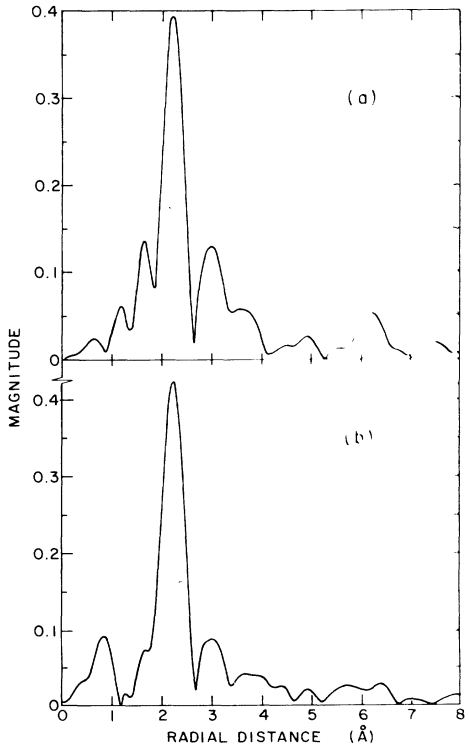

FIG. 9. Magnitude of the Fourier transform of k times the data of the tungsten L_3 edge in $2H$-WSe_2 shown in Fig. 5: (a) $\theta = 0°$, (b) $\theta = 47°$.

IV. Since the second peak is due to three shells and the EXAFS was only measured at two angles, there are no combinations of the present data for which the same procedure can be used on these shells. Also, for second and higher shells multiple scattering makes the relative amplitudes in Table IV less reliable.

The Fourier transforms of the W L_3-edge EXAFS in Fig. 5 are shown in Fig. 9. Again the transform is of $k\chi(k)$ but in this case a Hanning function cutoff was applied to the data to minimize truncation ripples in the transform. The large peak is centered at 2.23 Å and is due to the Se near-neighbor shell at 2.53 Å, which implies a phase shift of 0.30 Å. Since both of the transforms were taken over the same region in k space and the first peak is well resolved, the amplitude ratio for this peak can be read directly from the transforms. The amplitude at $\theta = 47°$ is 1.08 ± 0.02 times the amplitude at $\theta = 0°$. If the peak is due entirely to d final states, then from Table IV the amplitude ratio would be 1.14. The difference between this value and the measured ratio indicates that the cross term in Eq. (4) between s and d final states contributes significantly. In order to fit the measured amplitude dependence it is necessary to assume that $\langle 0|1\rangle/\langle 1|2\rangle = 0.20 \pm 0.06$. In determining this ratio the difference in the peak shifts introduced by the phase shifts of the two terms was assumed negligibly small. This is supported by the fact that the total peak shift, which is dominated by the d contribution, is 0.30 Å and from this one would estimate that the difference in peak shifts is ~0.05 –0.1 Å. The final s-states contribution to the total absorption at the L_3 edge is given by $\frac{1}{2}|\langle 0|1\rangle/\langle 1|2\rangle|^2 = 0.02$ of that of the final d states, justifying the neglect of the $|\langle 0|1\rangle|^2$ term in $\chi(k)$.

Also visible in these transforms is a small peak from the second shell of neighbors. The contribution from this shell shows a large angular dependence, with the amplitude at $\theta = 47°$ down by a factor of 0.67 ± 0.15, while the predicted value using the d term and cross term as just determined is 0.79 ± 0.04, consistent with the measured value. The amplitudes of this second-shell peak are not accurately determined because of interference from the strong neighboring shell and background noise.

VI. SUMMARY

In this paper we have shown how the plane polarization of the x-rays from a synchrotron source can be used to advantage in the study of anisotropic materials. The anisotropy is reflected both in the near-edge structure and its white line, and the EXAFS. The near-edge structure probes the local electronic density of states of the absorbing atom, and for Se in $2H$-WSe_2 we have observed the first true anisotropy. Previous anisotropy observed for Ta in $1T$-TaS_2 has been shown to be due to spurious effects. The EXAFS in $2H$-WSe_2 is also observed to exhibit anisotropy which can be well correlated to the known structural anisotropy of this material.

The anisotropy of the EXAFS at the L_3 edge has been experimentally and theoretically studied for the first time in detail. A general formulation of the orientation dependence of EXAFS, and the x-ray absorption coefficient in general, has been presented. The explicit form of the orientation dependence of EXAFS at $L_{2,3}$ edges has been presented. Comparison with experiment permits an estimate of the ratio of the s contribution to the d contribution to the total absorption above the L_3 edge of $2H$-WSe_2 to be 0.02.

This paper has emphasized several complications which are not universally recognized. The thickness effect must be accounted for in order to obtain accurate orientation dependences. There is no simple relationship between the near-edge structure and the electronic structure of the unperturbed material. In particular, one does not expect a quantitative comparison between a density of states calculation of the unperturbed material and the x-ray absorption near the edge. This is because the x-ray absorption is proportional to the local density of states at the core hole of the excited atom and not the average density of states of the unexcited material. However, some qualitative comparisons may hold such as the location of critical points in the density of states.

ACKNOWLEDGMENTS

We are most pleased to express our appreciation to Dr. Roger Pollak for supplying the single crystal of $1T$-TaS_2 which was grown by Merrill W. Shafer, and to Professor R. F. Frindt for supplying the $2H$-WSe_2 single crystal. The research in this paper was greatly aided by extensive contacts and conversations with our colleagues Farrel Lytle and Dale Sayers whose help is so pervasive that it is difficult to distinguish from one's own ideas.

*Supported by NSF Grant No. DMR73-02521 A02 and No. DMR73-07692, in cooperation with the Stanford Linear Accelerator Center and the U. S. ERDA.

[1]*X-Ray Spectroscopy*, edited by L. V. Azaroff (McGraw-Hill, New York, 1974), Chap. 6.

[2]M. Brown, R. E. Peierls, and E. A. Stern, Phys. Rev. B 15, 738 (1977).

[3]V. G. Bhide and M. K. Bahl, J. Phys. Chem. Solids 32, 1001 (1971).

[4]V. G. Bhide and B. A. Patki, Pramana 2, 290 (1974).

[5]E. A. Stern, D. E. Sayers, and F. W. Lytle, Phys. Rev. Lett. 37, 298 (1976).

[6]E. Alexander, B. S. Fraenkel, J. Perel, and K. Rabinovitch, Phys. Rev. 132, 1554 (1963); E. Alexander, J. Feller, B. S. Fraenkel, and J. Perel, Nuovo Cimento 35, 311 (1965); T. A. Boster and J. E. Edwards, J. Chem. Phys. 36, 3031 (1962); H. Fujimoto, Sci. Rep. Tohoku Univ. 49, 28 (1966); W. M. Weber, Physica (Utr.) 28, 689 (1962); 30, 2219 (1964); Phys. Lett 25A, 590 (1967); O. Brummer and G. Dröger, in *Rontgenspektren und chemische Bindung, Vorträge des internationalen Symposium, Leipzeg*, 1965, edited by A. Meisel (Physikalisch-Chemisches Institute der Karl-Marx-Universität, Leipzig, 1966), p. 35; Phys. Status Solidi 14, K175 (1966); W. M. Weber, Ph.D. thesis (University of Groningen, 1972) (unpublished).

[7]For an example of this approach, see L. D. Landau and E. M. Lifshitz, *Electrodynamics of Continuous Media* (Pergamon, New York, 1960).

[8]G. Beni and P. M. Platzman, Phys. Rev. B 14, 1514 (1976).

[9]E. A. Stern, Phys. Rev. B 10, 3027 (1974); P. A. Lee and J. P. Pendry, *ibid.* 11, 2795 (1975); P. A. Lee, *ibid.* 13, 5261 (1976).

[10]L. G. Parratt, C. F. Hempstead, and E. L. Jossem, Phys. Rev. 105, 1228 (1957).

[11]U. Fano and J. W. Cooper, Rev. Mod. Phys. 40, 441 (1968); A. Kotani and Y. Toyozawa, J. Phys. Soc. Jpn. 35, 1073 (1973); 35, 1082 (1973).

[12]L. L. Boyer, D. A. Papaconstantopoulos, and B. M. Klein, Phys. Rev. B 15, 3685 (1977).

[13]L. F. Mattheiss, Phys. Rev. B 8, 3719 (1973).

[14]R. A. Bromley, R. B. Murray, and A. D. Yoffe, J. Phys. C 5, 759 (1972).

[15]F. W. Lytle, D. E. Sayers, and E. A. Stern, Phys. Rev. B 15, 2426 (1977).